Journal of the European Ceramic Society **11** (1993) 523–532

Anisotropic Sintering Shrinkage in Injection-Moulded Composite Ceramics

S. J. Stedman, J. R. G. Evans

Department of Materials Technology, Brunel University, Uxbridge, Middlesex UB8 3PH, UK

&

R. J. Brook, M. J. Hoffmann

Max-Planck-Institute für Metallforschung, Pulvermetallurgisches Laboratorium, Heisenbergstrasse 5, D7000 Stuttgart 80, Germany

(Received 28 October 1991; revised version received 23 September 1992; accepted 20 November 1992)

Abstract

The sintering shrinkage of injection-moulded silicon nitride bars reinforced with 0–30 vol.% silicon carbide platelets or whiskers was measured in three orthogonal directions. The extent of shrinkage anisotropy is discussed in relation to inclusion aspect ratio, volume fraction and orientation.

Die Schrumpfung beim Sintern spritzgegossener Siliziumnitridbalken, die mit 0–30 Vol.% plättchenförmiger Siliziumkarbid-Teilchen oder -Whiskern verstärkt wurden, ist in drei orthogonalen Richtungen gemessen worden. Das Ausmaß der Schrumpfungsanisotropie wird im Zusammenhang mit dem Formfaktor der Einschlüsse, deren Volumenanteil und Orientierung diskutiert.

Le retrait au frittage de barreaux, moulés par injection, en nitrure de silicium renforcés avec 0–30 vol.% de plaquettes ou de trichites en carbure de silicium a été mesurée dans trois directions orthogonales. L'importance de l'anisotropie du retrait est discutée en termes de rapport d'aspect, de volume et d'orientation des inclusions.

1 Introduction

Composite ceramics are of interest for structural applications because they may offer enhanced fracture toughness[1–3] attributable to crack deflection and crack bridging at a whisker- or platelet–matrix interface.[4] Injection moulding of such materials is possible[5,6] and presents an effective procedure for the mass production of ceramic components.[7,8] However, in conventional injection moulding, anisotropic dispersoids undergo preferred orientation during mould filling.[5,6] For fibre–polymer composites which bear formal similarity to these systems the pattern of orientation in a moulded component is partly dependent on the mould and gate configuration[9] and on the machine conditions, notably injection speed.[10] Similar orientation patterns produced during the injection moulding of fibre-reinforced polymers have been studied extensively[11–13] but direct comparison with ceramic systems is impeded by the different flow behaviour of a matrix which consists of a highly filled ceramic suspension.

The arrangement of anisotropic dispersoids which is established at the moulding stage in turn leads to anisotropic dimensional changes during sintering, since the dispersoids act as impediments to shrinkage[6,14] so that shape is not retained during the final stage of the ceramic fabrication operation.

Three methods are available to characterise the orientation pattern in a fibre-reinforced body:

(i) Wide-angle X-ray diffraction (XRD).
(ii) Measurement of the elliptical axes of fibre sections observed on two polished surfaces.
(iii) Prediction from numerical models.

The first method is generally applicable to single-crystal fibres or whiskers and has been used to reveal preferred orientation in an extruded α-SiC whisker–polymer composite.[15] However, when applied to a metal matrix composite β-SiC–aluminium it was unsuccessful because of stacking faults in the whiskers.[16,17] An additional restriction is that attenuation limits the section thickness to 0·1–0·5 mm depending on the linear adsorption coefficient of the material.[18]

Journal of the European Ceramic Society 0955-2219/93/$6.00

The second method has also been used[19] but is strictly applicable to fibres of regular cross-section. The morphology of silicon carbide whiskers tends to vary widely[20] but nevertheless the method has been applied to the whisker orientation in an injection-moulded bar.[6] The silicon carbide whisker orientation pattern was related to the distortion of the body during subsequent sintering.

The development of predictive methods such as that of Folgar & Tucker[21] would enable the rapid assessment of mould designs and machine parameters, although this has yet to be fully developed for fibre-reinforced polymers. Furthermore, techniques have recently become available for the management of fibres in injection moulding and these offer considerable scope for ceramic and metal matrix composite fabrication.[22,23]

In the case of composite ceramics, the addition of non-sintering inclusions hinders sintering[24-32] and transient stresses are developed as different regions of the assembly densify at different rates. Although, in principle, full density may still be achieved, the sintering time is considerably extended.[33] The degree of hindrance is influenced by the size and the volume loading of the non-sintering inclusions.[34]

In practice, silicon carbide whisker composites sinter to lower final densities than silicon carbide particulate composites with the same fraction of second phase, showing that the aspect ratio of inclusions influences the degree of hindrance.[14,34] Furthermore, the high aspect ratio of silicon carbide whiskers may allow network formation even at relatively low volume loadings.[35] The reality of the stresses introduced by differential shrinkages has been elegantly shown by the work of Ostertag[36] where warpage in components containing asymmetric distribution of fibre inclusions has been observed.

The practical difficulties caused by orientated anisotropic non-sintering inclusions has been illustrated.[6,14,37] Aerofoil sections prepared from a silicon carbide–silicon nitride composite showed severe distortion on sintering.[6]

The perceived advantages of tougher composite ceramics[38-40] may only be realised if the parts can be successfully produced to high dimensional tolerances to avoid expensive post-densification machining. The prediction of the anisotropic sintering shrinkage in terms of the non-sintering inclusion volume loading, aspect ratio and orientation pattern is thus of practical interest.

2 Experimental Details

Silicon carbide whiskers (Tateho Chemical Industries, Ako-Shi, Japan, Grade SCW #1) or silicon carbide platelets (American Matrix Inc., Knoxville, USA, grade −200, +325 and −325) were mixed with silicon nitride powder (Showa Denko, Japan, Grade NU-10) with sintering aids (5 wt% Y_2O_3 concentrate, Rare Earth Products, UK and 5·5 wt% Al_2O_3, A16, Alcoa, UK). The suspensions were premixed with organic binders in a Henschel high-speed non-refluxing mixer and subsequently compounded with a Betol TS40 twin screw extruder operating at 100 rpm with barrel temperatures 210, 215, 225, 215°C feed to exit. The binder system was isotactic polypropylene (ICI, Welwyn Garden City, UK, grade GY545M), microcrystalline wax (Astor Chemicals, West Drayton, UK, grade 1865Q) and stearic acid in the weight ratios of 6:2:1. The compositions are given in Table 1 based on the mean of four ashing experiments assuming the organic constituents to be present in the proportions in which they were weighed out. One set of samples of the silicon carbide whisker composite were collected after compounding and extrusion through a 6 mm diameter die.

The other compounded blends were injection

Table 1. Compositions of the injection moulding suspensions

Sample number	*Inclusion type*	*Volume ratio inclusion: matrix*	*Total ceramic volume fraction*[a]
W7	Whiskers	20:80	50
W10	Whiskers	23:77	51
W11	Whiskers	27:73	49
W12	Whiskers	30:70	50
C5	None	0:100	56
C6	Platelets (fine)[b]	10:90	56
C3	Platelets (fine)[b]	20:80	54
C8	Platelets (fine)[b]	30:70	56
C7	Platelets (coarse)[c]	10:90	56
C4	Platelets (coarse)[c]	20:80	56
C9	Platelets (coarse)[c]	30:70	56

[a] Based on ashing results.
[b] Fine platelets −325 mesh.
[c] Coarse platelets −200, +325 mesh.

moulded with either a Manumold Model 77 Mk.4 (whisker composites) or a Sandretto 6GV/50 (platelet composites). The organic binder was removed by slow heating in air (40°C/h to 120°C, 1°C/h to 350°C, 10°C/h to 550°C) and the specimens were sintered in a powder bed at 40°C/min to 900°C, 20°C/min to 1850°C or 1950°C where they were held for 30 min. A nitrogen over-pressure of 0·6–2 MPa was applied. The anisotropic shrinkage was calculated to be the linear sintering shrinkage in the orientated direction (the length direction of the bars) divided by the shrinkage in the transverse direction. The dimensions were measured after binder removal and after sintering. Additionally, sections were cut from the centre of the injection-moulded 20 vol.% platelet composite and a silicon nitride injection-moulded bar. The shrinkages in length, depth and width directions were measured using a dynamic dilatometer attached to a graphite heated furnace (Astro Industries, USA, Model No. 1000-4560-FP20). The heating rate was 20°C/min to 1850°C under 0·1 MPa nitrogen pressure.

Selected samples were surface ground, lapped, polished and etched in boiling phosphoric acid for 2–5 min and examined by optical and scanning electron microscopy using a Cambridge S200. Samples were also prepared by isostatic pressing at 200 MPa after mixing the powders in a Turbula mill (Model T2C from Willy, A. Bachofen AG, Basel, Switzerland) for 4 h at room temperature in isopropanol with 5 mm diameter silicon nitride media.

3 Results and Discussion

3.1 Effect of silicon carbide additions on final sintered density

The whiskers as they were received are shown in Fig. 1. During the mixing procedure, considerable whisker length degradation takes place, the large whiskers being particularly susceptible to damage. The final average length is in the 8–10 μm region.[41]

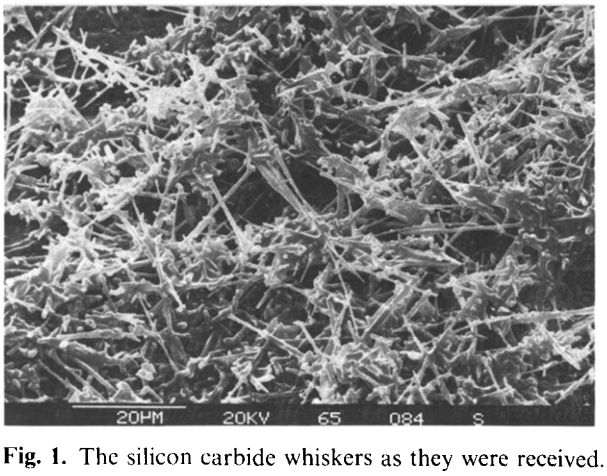

Fig. 1. The silicon carbide whiskers as they were received.

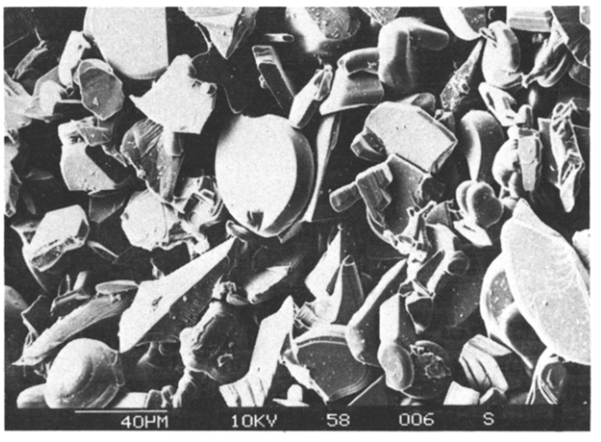

Fig. 2. Silicon carbide platelets (coarse).

Figure 2 shows the coarse silicon carbide platelets which present considerable irregularity of shape, size and thickness.

Throughout this work the weight fraction of sintering additions based on silicon nitride was kept constant so that an increase in silicon carbide content corresponded to an overall decrease in the fraction of sintering additives based on the total ceramic content, as shown in Table 2. Since the liquid-phase sintering additives do not directly enhance the densification of silicon carbide, any decrease in the final sintered density of composites as the silicon carbide fraction is increased can be attributed to the influence of the inclusions. Figure 3 shows that the deleterious effect of whiskers is considerably greater than that of platelets for a given inclusion volume fraction. For the whisker composites the initial total ceramic content was 50 vol.% and it can be seen that a volume shrinkage on binder removal and sintering of only 21% has occurred for the 30 vol.% whisker composite. For the platelet composites the initial volume loading was 56 vol.%.

The final sintered densities of the injection-moulded and the extruded whisker composites are similar. The platelet composites achieve a higher final density because of the lower aspect ratio of the

Table 2. Sintering additives as a percentage by weight of the ceramic content

Type of inclusion	*Inclusion (vol.%) based on ceramic*	*Sintering additions (wt%) based on total ceramic*
Whiskers	0	10·5
Whiskers	20	8·4
Whiskers	23	8·1
Whiskers	27	7·7
Whiskers	30	7·4
Platelets	10	9·5
Platelets	20	8·4
Platelets	30	7·4

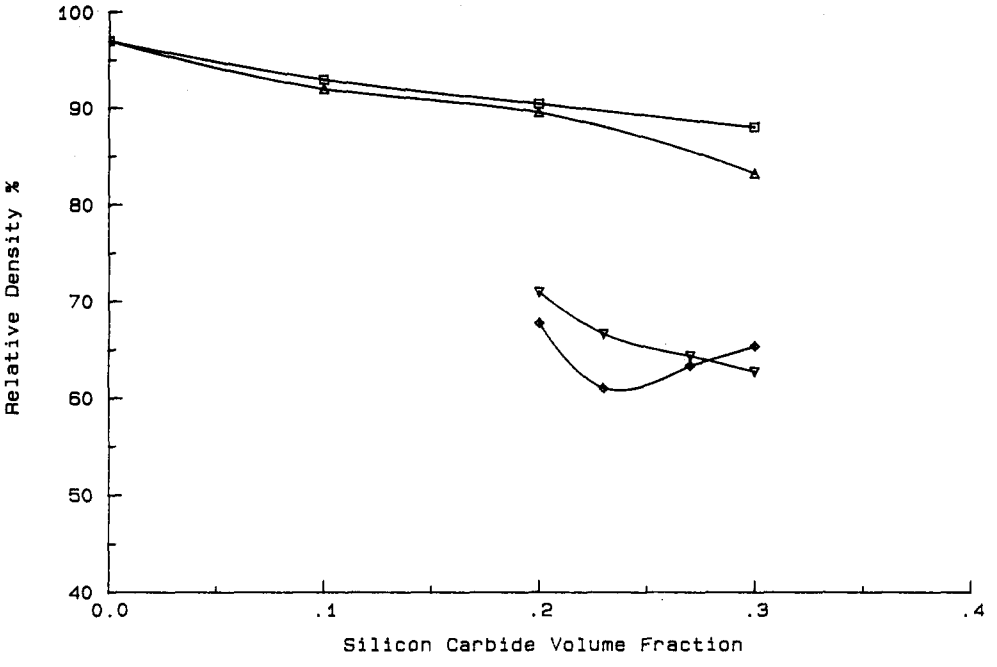

Fig. 3. Effect of silicon carbide inclusion morphology at various loadings on sintered relative density of injection-moulded samples. ▽, Injection-moulded whisker composite; ◇, extruded whisker composite; △, injection-moulded coarse platelets and □, fine platelets. Sintering temperature 1950°C, 30 min, 0·6 MPa N_2. Initial relative density: whisker composite 50%, platelet composite 56%. The largest 95% confidence limit calculated from a '*t*' distribution for measurements on up to four samples represents 5% relative density.

non-sintering inclusions, highlighting the relevance of inclusion morphology to the fabrication process.

The extent to which this situation can be remedied by increased sintering time and nitrogen over-pressure is shown in Table 3, which indicates that injection-moulded samples containing 30 vol.% fine platelets can be pressureless sintered to 92% relative density after 2 h at 1850°C. Prolonged sintering times may permit grain growth, while high nitrogen over-pressures may encourage the nitridation of silicon carbide, and these factors considerably restrict the possible variations in sintering conditions.[42] Table 3 also shows that platelet size influences densification independently of volume fraction. Thus the composites containing fine platelets reach a high density for the same sintering conditions. Figure 4 shows that higher theoretical densities are obtained from injection-moulded fine platelet composites than from the same compositions prepared by cold isostatic pressing and after firing under the same conditions. This can be attributed to the preferred orientation of platelets which tends to result from mould filling in injection moulding but

Table 3. Effect of SiC platelet size on sintered relative density of composites prepared by injection moulding

SiC volume fraction	*Relative density (%)*			
	A		*B*	
	Coarse	*Fine*	*Coarse*	*Fine*
0	98	98	94	94
0·1	95	96	90	92
0·2	96	94	86	85
0·3	85	92	81	85

A: Sintered at 1850°C for 120 min under 1 MPa N_2.
B: Sintered at 1850°C for 30 min under 0·1 MPa N_2.

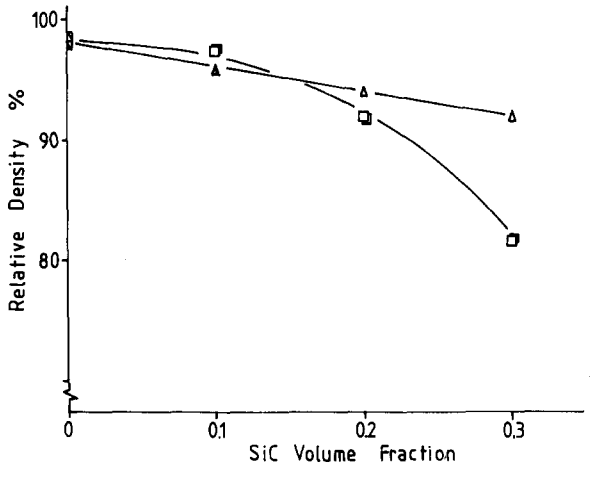

Fig. 4. The effect of fabrication route on relative density for Δ injection-moulded and □, isostatically pressed composites containing fine platelets sintered at 1850°C for 120 min under 1 MPa N_2.

to be highly random for the pressed samples, and this is discussed. There is also a significant influence of silicon carbide platelet fraction on the weight loss during sintering (Fig. 5). A slight weight loss is quite normal during the sintering of silicon nitride but the weight gain observed at high silicon carbide contents can be attributed to the conversion of silicon carbide to nitride under the nitrogen atmosphere:

$$3SiC + 2N_2 \rightarrow Si_3N_4 + 3C$$

Under the assumption that SiC inclusions completely transform to Si_3N_4 this reaction is responsible for a 14% weight increase if carbon remains in the system or a 5% increase if traces of oxygen-containing species render the free carbon mobile. The extent of reaction, which was more pronounced under high nitrogen over-pressures[42] can be seen in the micrographs shown in Fig. 10.

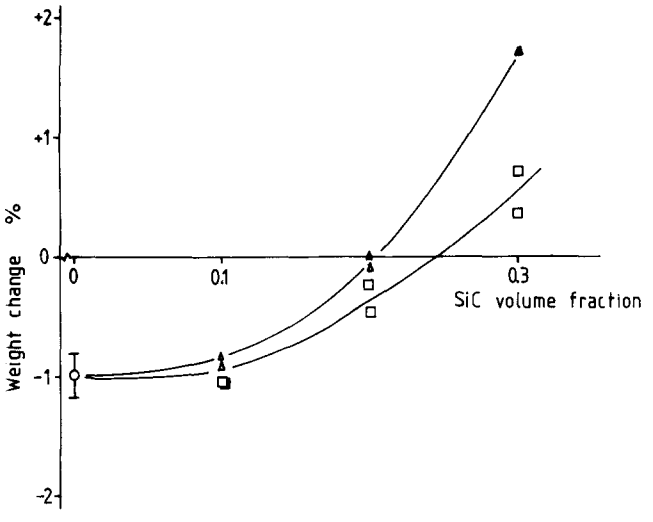

Fig. 5. The influence of silicon carbide platelet fraction on the sintering weight change for cold isostatically pressed samples; △, coarse platelets; □, fine platelets.

3.2 Anisotropic sintering shrinkage

In order to characterise the anisotropic shrinkage, a relative shrinkage parameter for the injection-moulded platelet or whisker composites was defined as the ratio of shrinkage in the longitudinal and transverse directions of the injection-moulded or extruded bar. The results in Fig. 6 can be interpreted in terms of the preferential alignment of whiskers with their axes in the direction of the length of the bar. Similarly, the plane of the platelets tends to be parallel to the longitudinal direction of the bar. This is similar to the experimental orientation patterns for injection-moulded fibre-reinforced polymers. The actual orientation is such that platelets arrange themselves parallel to the surfaces of the bar and this gives rise to concavity of the surfaces on sintering. The exact measurement of shrinkage was difficult and the results in Fig. 6 reflect the overall shrinkage anisotropy. This partly explains the upturn of the curve for the platelets at 30 wt% wherein the high concentration of platelets leads to greater concavity of the surfaces.

The extruded whisker composites present much greater anisotropic sintering shrinkage. Extrusion of the suspensions leads to much greater whisker orientation and therefore lower shrinkage ratios. Similarly, the effect of inclusion morphology is clear; the platelets present the least shrinkage anisotropy. There is little difference between the relative shrinkage parameter for the coarse and fine platelets (Fig. 6) and this reflects the similarity in aspect ratio. Measurements of 50 platelets of each indicate aspect ratios of 0·25–0·33 for the small platelets and 0·2–0·33 for the larger platelets. Although the shrinkage on debinding is usually less than 1% linear, the sintering shrinkage (typically 15–20% linear) gives rise to significant variations in the dimensional tolerance of components when the ratios in Fig. 6 are applied to complex geometries and severely undermines the usefulness of conventional injection moulding for composite ceramics. Procedures have been developed to control the orientation of fibres in polymer composites by using multigated cavities and inducing reciprocating flow within the cavity immediately before solidification.[22,23] This should allow preferred orientation to be achieved in composite ceramics but mould dimensions would still have to be calculated for non-uniform shrinkage on subsequent sintering.

The progress of anisotropic shrinkage during sintering was followed by dilatometry for an unreinforced silicon nitride bar and a 20 vol.% silicon carbide fine platelet composite bar. For the unreinforced bar the shrinkage curves in the length, width and depth directions are shown in Fig. 7 and,

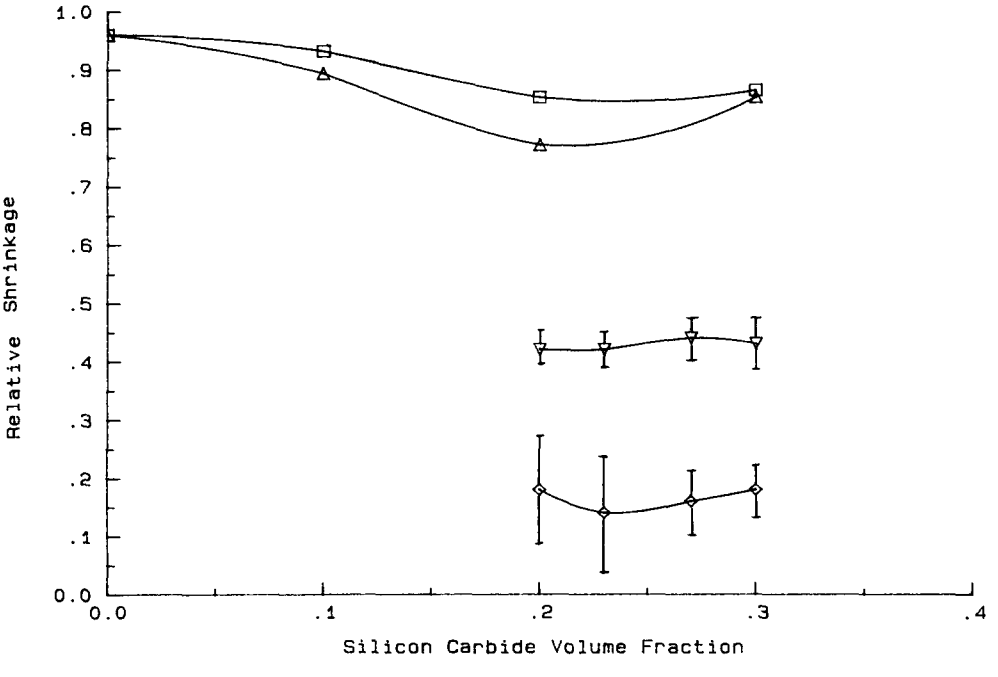

Fig. 6. Relative shrinkage parameter for injection-moulded bars sintered at 1950°C for 30 min under 0·6 MPa N_2. △, Coarse platelets; □, fine platelets; ▽, whiskers (injection-moulded); ◇, whiskers (extruded). Error bars represent 95% confidence limits calculated from a '*t*' distribution for measurements on up to four samples.

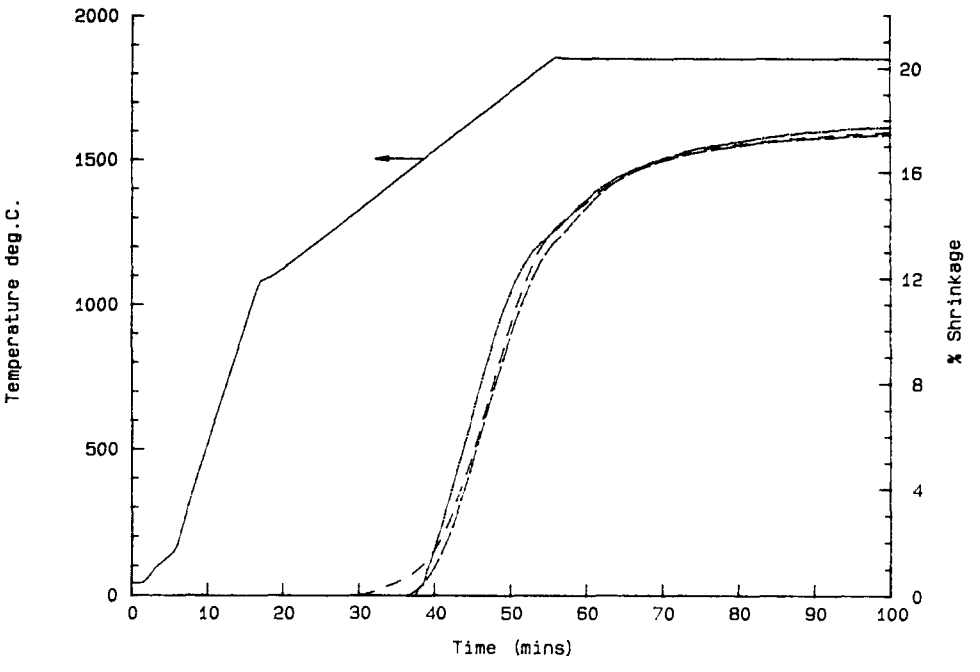

Fig. 7. Dilatometric shrinkage curves for a section of an injection-moulded bar containing no non-sintering inclusions (nitrogen pressure: 0·1 MPa); – – –, length; ———, width; —·—·—, depth.

as expected, are almost coincident. The corresponding curves for the platelet-reinforced bar show consistent differences in the shrinkage in the length, width and thickness directions (Fig. 8). Anisotropy of shrinkage manifests itself at an early stage and the curves for the three orthogonal directions are similar in form throughout the sintering process.

3.3 Optical microscopy

The high optical reflectivity of silicon carbide means that the platelets are clearly visible in the reflected light microscope. Figure 9 shows the full cross-section of an injection-moulded bar with 20% coarse platelets. No evidence of segregation of platelets could be detected by optical microscopy. The normal axes of platelets lie in the plane of the paper and Fig. 10 shows the orientation of the plane of the platelets with respect to the width and depth directions, which forms an elliptical pattern in the section of the bar. The fact that the platelet normals lie perpendicular to the longitudinal axis of the bar accounts for the impeded shrinkage in the longitudinal directions, but Figs 9 and 10 also account for the impeded shrinkage in the width direction compared to the depth direction. A high proportion of platelets are aligned with the normals perpendicular to the width direction, that is to say that they lie parallel to the major axes of the ellipses in Fig. 10. Shrinkage in the depth direction suffers the least impediment because it is parallel to the platelet normals.

This pattern also explains the concavity of the

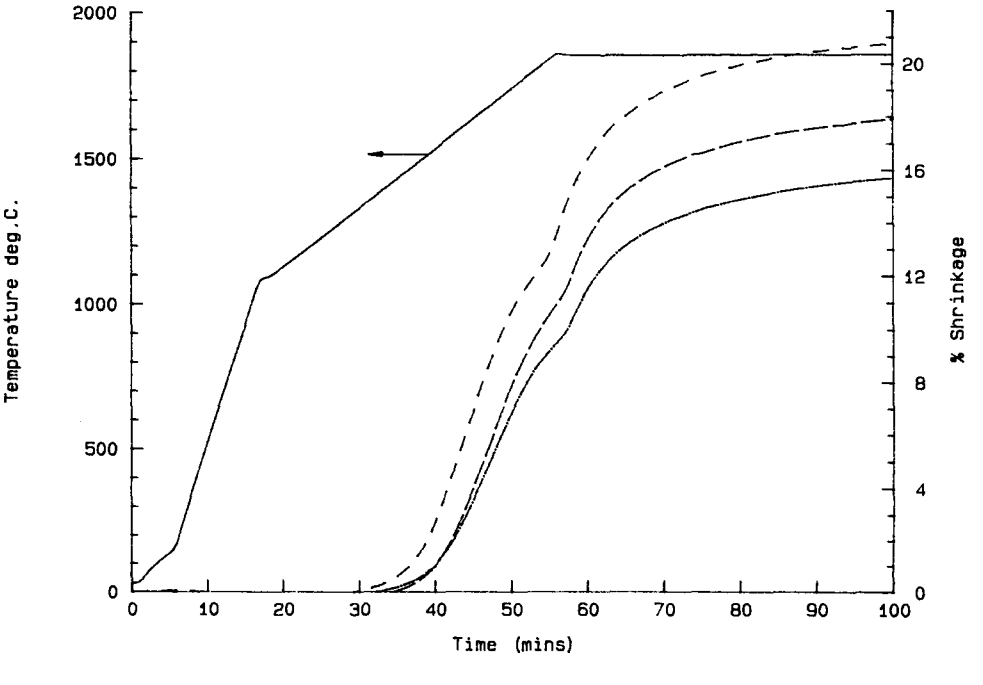

Fig. 8. Dilatometric shrinkage curves for a section of an injection-moulded bar containing 20 vol.% silicon carbide platelets (nitrogen pressure: 0·1 MPa); —·—·—, length; – – –, width; – – –, depth.

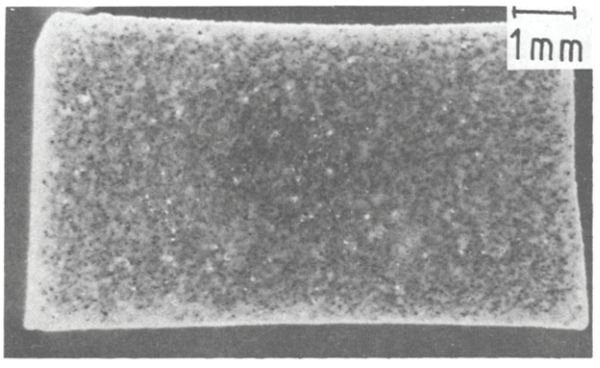

Fig. 9. Optical micrograph of the cross-section of a sintered injection-moulded bar containing 20 vol.% coarse silicon carbide platelets.

faces of the bar shown in Fig. 9. Shrinkage is least impeded near the mid-planes of the bar. This is not caused by density variations in bars which are negligible[43] nor to shrinkage during moulding which was not evident in the as moulded state. The orientation is seen more clearly in Fig. 11 which shows the alignment of platelets in sections of Fig. 9 and the schematic cross-section in Fig. 10.

3.4 A simplified model for shrinkage anisotropy

Consider an hexagonal prism of side s and length L surrounded by a layer of constant thickness t, representing the unsintered matrix. If the prism has a

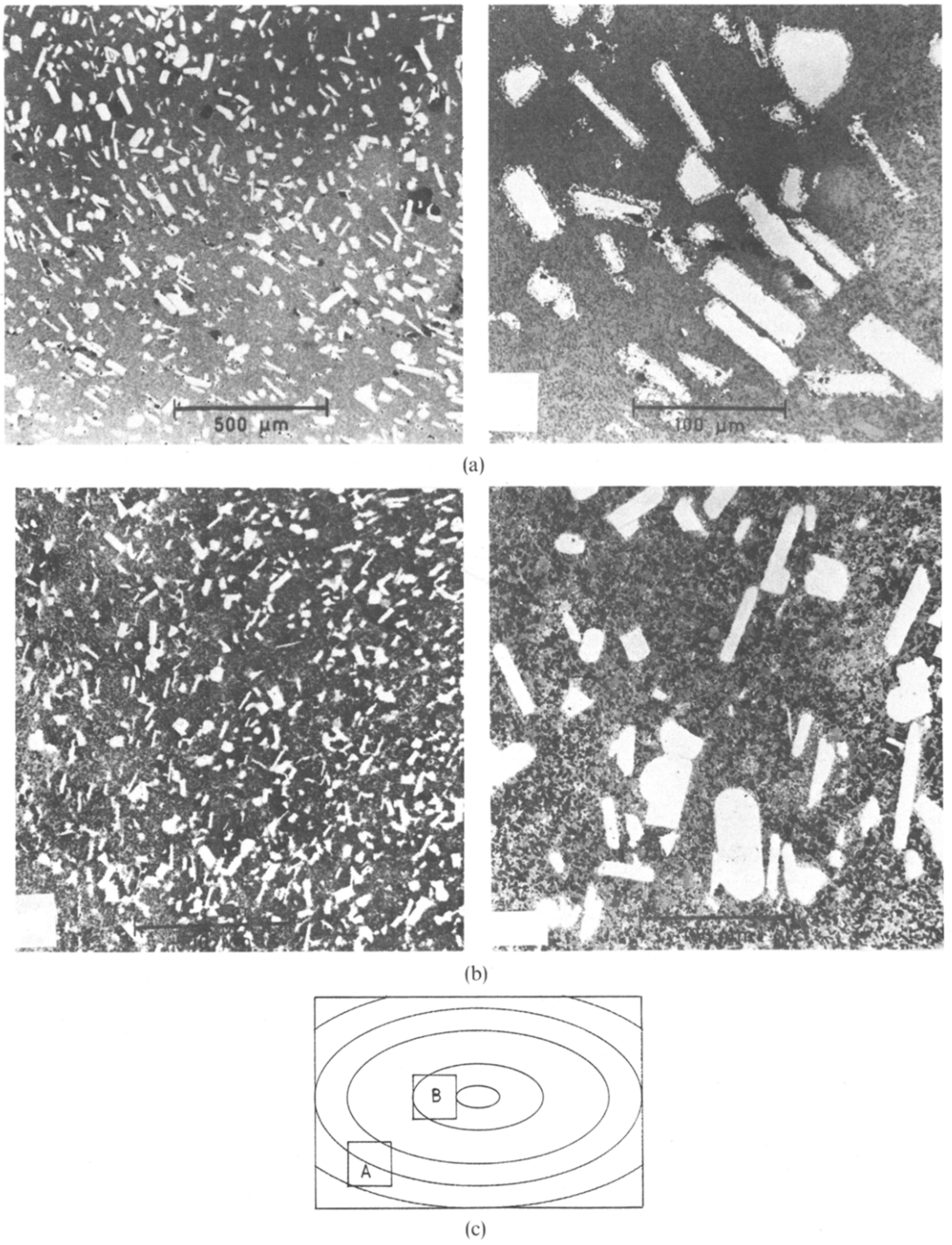

Fig. 10. Optical micrographs of the transverse section of injection-moulded bars containing 20 vol.% coarse silicon carbide platelets at positions defined in (c) which shows a schematic diagram of the orientation of platelets in the transverse section.

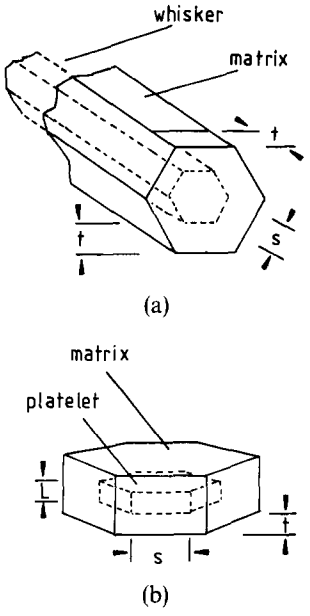

Fig. 11. The geometry used in the model for estimating the relative shrinkage parameter for (a) the case of whiskers $A > 1$ and (b) the case of platelets $A < 1$.

high aspect ratio, it can be considered to represent a whisker. A platelet is represented by a low aspect ratio prism. The matrix is considered to sinter to full density around the inclusion. The hexagonal prisms and their coatings efficiently fill space. Thus the transverse and longitudinal shrinkages of each unit correspond to the macroscopic values. The geometry is shown in Fig. 12.

In sintering to high density, it is assumed that the coating shrinks normal to the surface of the inclusion. This is the same assumption that has been made in the treatment of viscous sintering on a rigid

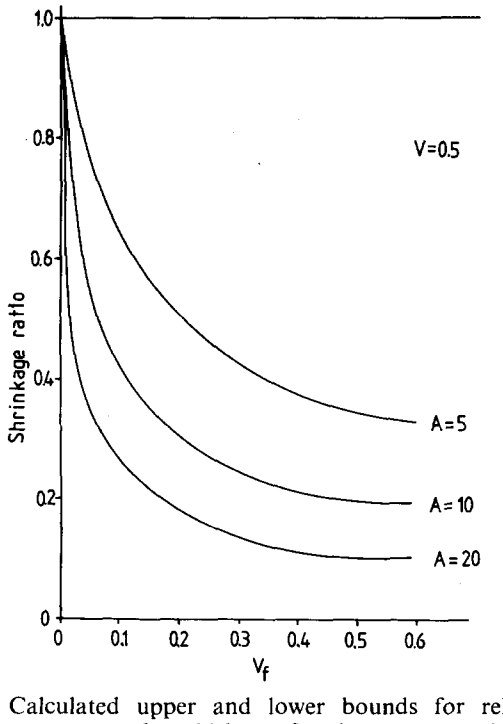

Fig. 12. Calculated upper and lower bounds for relative shrinkage parameter for whiskers of various aspect ratios for $V = 0{\cdot}5$ at a range of volume fractions of inclusion V_f.

substrate by Scherer & Garino.[44] In the present instance, with inclusions of finite dimensions, shear stresses are generated parallel to the inclusion surface. For this initial treatment, however, it will be assumed that the bonding between the matrix and the inclusion is of a strength such that shear relaxation at the interface does not occur. Shrinkage in the coating is accordingly normal to the inclusion surface.

If s is the length of the side of the prism, then its volume is $\frac{3}{2}\sqrt{3}s^2L = 2{\cdot}598s^2L$ and the distance across the flats is $2s\cos 30 = 1{\cdot}7321s$. The aspect ratio A is given by

$$A = L/1{\cdot}7321s \tag{1}$$

The new side length of the coated prism is $s + 1{\cdot}547t$.

If the void volume fraction in the matrix before firing is V, then the prefired relative density of the matrix is $(1 - V)$ and the volume fraction V_f of dispersoids based on the volume of ceramic is

$$V_f = \frac{s^2L}{(1-V)(s+1{\cdot}1547t)^2(L+2t)+s^2LV} \tag{2}$$

For various values of V_f this cubic in t can be solved numerically.

The linear shrinkages in the transverse and longitudinal directions can then be found as follows. Since the coating cannot shrink in the length direction of the prism, the void space is taken up by shrinkage in the thickness direction irrespective of the aspect ratio. From a consideration of the volume of the coating on the sides of the prism, before and after sintering to full density a new value of thickness t' can be found as follows:

$$t' = \frac{\sqrt{(1-V)(2{\cdot}309ts + 1{\cdot}333t^2) + s^2} - s}{1{\cdot}1547} \tag{3}$$

The linear shrinkage in the transverse direction is found from:

$$\left(\frac{\Delta L}{L_0}\right)_T = \frac{2(t-t')}{1{\cdot}732s} + 2t \tag{4}$$

The shrinkage in the longitudinal direction can be derived under similar conditions. The end caps, which overlap the coating on the sides of the prism, are considered to shrink only in the length direction, providing a new coating thickness t'' given by:

$$t'' = t(1 - V) \tag{5}$$

The longitudinal shrinkage is then found from:

$$\left(\frac{\Delta L}{L_0}\right)_L = 1 - \frac{L+2t''}{L+2t} \tag{6}$$

This simplified geometry does not properly treat the region of matrix adjacent to the corners of the prism and this is reflected in a discrepancy in the

volumetric shrinkages calculated from the volume fractions of ceramic on the one hand and from the longitudinal and transverse shrinkages on the other, for the case of sintering to full density. This leads to errors which are most pronounced at low values of V_f and A.

When applied to the case where all dispersoids are uniformly orientated and with the thickness t constant, the model can be used to give a lower bound estimate of shrinkage ratio, displaying the influences of A, V and V_f. However, the shrinkage anisotropy is sensitive to the arrangement of the dispersoids in the matrix. Thus if, instead of a coating of uniform thickness, the hexagonal prisms reside in a box which presents the same aspect ratio as the inclusions themselves, an upper bound result is obtained for which:

$$\frac{L+2u}{1{\cdot}732s+2t}=\frac{L}{1{\cdot}732s}=A \qquad (7)$$

where u is the end cap thickness. From this $u/t=A$ and the shrinkage ratio is unity for all aspect ratios, volume fractions of inclusion and matrix relative densities. It should be noted that the longitudinal direction in the experimental results is defined in terms of the injection-moulded or extruded bar, while the L direction in the model is defined in terms of the geometry of the hexagonal prism. Therefore the model predicts relative shrinkage parameter as greater than unity for platelets, in contrast to the experimental situation.

The relative shrinkage parameters which result from this model are shown in Fig. 12 for the case of $V=0{\cdot}5$ and for various aspect ratios of inclusion. This should be compared with Fig. 6 in which the results for the extruded whisker composites, in which a high level of preferred orientation prevails, compare well with the predicted curves. In fact, the whiskers contain a wide variation in aspect ratio with an average value of $A=8$. Inserting the more accurate $V=0{\cdot}584$, $V_f=0{\cdot}3$ and $L=8\,\mu$m, the latter quality representing a mean with wide variation, the relative shrinkage parameter is predicted to be 0·25, compared with the measured value of 0·18 in Fig. 6.

4 Conclusions

In silicon nitride–silicon carbide composites with a given volume fraction of silicon carbide inclusions, whiskers inhibit the densification of the composite to a much greater extent than silicon carbide platelets. Final sintered densities of 92–93% theoretical can be achieved with up to 20 vol.% platelets after 2 h without hot isostatic pressing.

Silicon carbide whiskers of volume loadings in the 20–30 vol.% region can ensure very high anisotropic shrinkage in injection-moulded or extruded shapes. The anisotropic sintering shrinkage of injection-moulded silicon carbide platelet–silicon nitride composites was less than that for whisker composites but was nevertheless sufficient to impair dimensional control. Thus the orientation pattern of non-sintering inclusions can give rise to shape distortion in a process intended to allow the retention of complex shape. The degree of shrinkage anisotropy increases with inclusion volume loading, inclusion aspect ratio and can be expected to increase with matrix shrinkage. A simplified geometrical model has been proposed to illustrate the anisotropic shrinkage resulting from unequiaxed inclusions.

Acknowledgements

One of the authors (SJS) is grateful to the Deutscher Akademischer Austauschdienst for support as a visiting scholar at the Max Planck Institute for Metals Research.

References

1. Wei, G. C. & Becher, P. F., Development of SiC-whisker reinforced ceramics. *Amer. Ceram. Soc. Bull.*, **64** (1985) 298–304.
2. Lange, F. F., Effect of microstructure on the strength of Si_3N_4–SiC composite system. *J. Amer. Ceram. Soc.*, **56** (1973) 445–50.
3. Buljan, S. T. & Sarin, V. K., Silicon nitride-based composites. *Composites*, **18** (1987) 99–106.
4. Homeny, J., Vaughin, W. L. & Faber, M. K., Processing and mechanical properties of SiC-whisker–Al_2O_3-matrix composites. *Amer. Ceram. Soc. Bull.*, **67** (1987) 333–8.
5. Kandori, T., Kobuyashi, S., Wada, S. & Kamigaito, O., SiC whisker reinforced Si_3N_4 composites. *J. Mat. Sci. Lett.*, **6** (1987) 1356–8.
6. Neil, J. T. & Norris, D. A., Whisker orientation measurements in injection moulded Si_3N_4–SiC composites. Gas Turbine and Aeroengine Congress, Amsterdam, The Netherlands, 6–9 June 1988, ASME 88-GT-193.
7. Edirisinghe, M. J. & Evans, J. R. G., Review: fabrication of engineering ceramics by injection moulding. I. Materials selection. *Int. J. High Tech. Ceram.*, **2** (1986) 1–31.
8. Edirisinghe, M. J. & Evans, J. R. G., Review: fabrication of engineering ceramics by injection moulding. II. Techniques. *Int. J. High Tech. Ceram.*, **2** (1986) 249–78.
9. Crowson, R. J., Folkes, M. J. & Bright, P. F., Rheology of short glass fibre-reinforced thermoplastics and its application to injection moulding. I. Fibre motion and viscosity measurement. *Polym. Eng. Sci.*, **20** (1980) 925–33.
10. Isayer, A. I., Orientation, residual stresses and volumetric effects in injection moulding. In *Injection and Compression Moulding Fundamentals*, ed. A. I. Isayer. Marcel Dekker, NY, 1987, pp. 227–328.
11. McGee, S. N. & McCullough, R. L., Characterization of fibre orientation in short fibre composites. *J. Appl. Phys.*, **55** (1984) 1394–403.
12. Darlington, M. W., Gladwell, B. K. & Smith, G. R., Structure and mechanical properties of injection moulded discs of glass fibre reinforced polypropylene. *Polymer*, **18** (1977) 1269–74.

13. Goettler, L. A., Controlling flow orientation in moulding of short fibre compounds. *Modern Plastics*, **47** (1970) 140–6.
14. Hoffmann, M. J., Nagel, A., Greil, P. & Petzow, G., Slip casting of SiC-whisker reinforced silicon nitride. *J. Amer. Ceram. Soc.*, **72** (1989) 765–9.
15. Schierding, R. G., Measurement of whisker orientation by X-ray diffraction. *J. Composite Mater.*, **2** (1968) 448–52.
16. Diricher, A., Lare, P. & Hahn, H., Silicon carbide whisker metal matrix composites. 1967, AFML-TR-67321.
17. Keppe, R. A. & Subbana, S. N., Development of orientated silicon carbide bodies. 1967, Appendix to Final Report No. AFML-TR-67321.
18. Cullity, B. D., *Elements of X-Ray Diffraction.* Addison-Wesley, 1978, p. 176.
19. Folkes, M. J., *Short Fibre Reinforced Thermoplastics.* Research Studies Press, Wiley, NY, 1982, pp. 85–6.
20. Yeh, H., Schiele, J., Karesek, K. & Bradley, S., Development of ceramic matrix composites for application in the ceramic technology for advanced heat engines. ORNL/Sub/85-22008/1.
21. Folgar, F. & Tucker, C. L., Orientation behaviour of fibers in concentrated suspensions. *J. Reinf. Plast. Compos.*, **3** (1984) 98–119.
22. Allan, P. S. & Bevis, M. J., Multiple live feed injection moulding. *Plast. Rubb. Prc. Appl.*, **7** (1987) 3–10.
23. Allan, P. S. & Bevis, M. J., The development and application of the multi life-feed moulding process for the production of injection mouldings containing laminated and other specific fibre orientation distributions. In *PNL 3rd Euro. Conf. on Composite Materials.* Elsevier, London, 1989, pp. 375–80.
24. Messing, G. L. & Onoda, G. Y., Sintering of inhomogeneous powder mixtures. *J. Amer. Ceram. Soc.*, **64** (1981) 468–72.
25. Evans, A. G., Considerations of inhomogeneity effects in sintering. *J. Amer. Ceram. Soc.*, **65** (1982) 497–501.
26. Raj, R. & Bodia, R. K., Sintering behaviour of bi-modal powder compacts. *Acta Metall.*, **32** (1984) 1003–19.
27. Bordia, R. K. & Raj, R., Analysis of sintering of a composite with a glass or ceramic matrix. *Comm. Amer. Ceram. Soc.*, **69** (1986) C55–C57.
28. Hsueh, C. H., Evans, A. G., Cannon, R. M. & Brook, R. J., Viscoelastic stresses and sintering damage in heterogeneous powder compacts. *Acta Metall.*, **34** (1986) 927–36.
29. DeJonghe, L. C., Rahaman, M. N. & Hsueh, C. H., Transient stresses in bimodal compacts during sintering. *Acta Metall.*, **34** (1986) 1467–71.
30. DeJonghe, L. C. & Rahaman, M. N., Sintering stress of homogeneous and heterogeneous powder compacts. *Acta Metall.*, **36** (1988) 223–9.
31. Hsueh, C. H., Sintering of whisker-reinforced ceramics and glasses. *J. Amer. Ceram. Soc.*, **71** (1988) C442–C444.
32. Scherer, G. W., Viscous sintering with a pore-size distribution and rigid inclusions. *J. Amer. Ceram. Soc.*, **71** (1988) C447–C448.
33. Lange, F. F., Constrained network model for predicting densification behaviour of composite powders. *J. Mater. Res.*, **2** (1987) 59–65.
34. Weiser, M. W. & DeJonghe, L. C., Inclusion size and sintering of composite powders. *J. Amer. Ceram. Soc.*, **71** (1987) C125–C127.
35. Holm, E. A. & Cima, M. J., Two-dimensional whisker percolation in ceramic matrix–ceramic whisker composites. *J. Amer. Ceram. Soc.*, **72** (1989) C303–C305.
36. Ostertag, C., Technique for measuring stresses which occur during sintering of a fibre-reinforced ceramic composite. *J. Amer. Ceram. Soc.*, **70** (1987) C355–C357.
37. Buljan, S. T., Baldoni, J. G., Neil, J. & Zilberstein, G., Dispersoid-toughened silicon nitride composites. Final Report, ORNL/Sub/85-22011/1.
38. Becher, P. F., Hsueh, C. H., Angelini, P. & Tiegs, T. N., Toughening behaviour in whisker-reinforced ceramic matrix composites. *J. Amer. Ceram. Soc.*, **71** (1988) 1050–61.
39. Becher, P. F., Tiegs, T. N., Ogle, J. C. & Warwick, W. H., Toughening of ceramics by whisker reinforcement. In *Fracture Mechanics of Ceramics*, Vol. 7, ed. R. C. Bradt, A. G. Evans, D. P. Hasselman & F. F. Lange. Plenum Press, NY, 1986, pp. 61–73.
40. Tiegs, T. N. & Becher, P. F., Whisker reinforced ceramics composites. In *Tailoring of Multiphase and Composite Ceramics*, ed. R. Tressler, G. Messing, C. Panton & R. Newman. Plenum Press, NY, 1986, pp. 639–47.
41. Stedman, S. J., Evans, J. R. G. & Woodthorpe, J., Whisker length degradation during the preparation of composite ceramics for injection moulding. *J. Mater. Sci.*, **25** (1990) 1025–32.
42. Nickel, K. G., Hoffmann, M. J., Greil, P. & Petzow, G., Thermodynamic calculations for the formation of SiC-whisker reinforced Si_3N_4. *Adv. Ceram. Mater.*, **3** (1988) 557.
43. Thomas, M. S. & Evans, J. R. G., Non-uniform shrinkage in ceramic injection moulding. *Brit. Ceram. Trans. J.*, **87** (1988) 22–6.
44. Scherer, G. W. & Garino, T., Viscous sintering on a rigid substrate. *J. Amer. Ceram. Soc.*, **68** (1985) 216–20.